



HAL
open science

The oxygen isotopic composition ($^{18}\text{O}/^{16}\text{O}$) in the dust of comet 67P/Churyumov-Gerasimenko measured by COSIMA on-board Rosetta

John Paquette, C. Engrand, J Hilchenbach, Nicolas Fray, J Stenzel, J Silen, J Rynö, J Kissel, The Cosima Team

► To cite this version:

John Paquette, C. Engrand, J Hilchenbach, Nicolas Fray, J Stenzel, et al.. The oxygen isotopic composition ($^{18}\text{O}/^{16}\text{O}$) in the dust of comet 67P/Churyumov-Gerasimenko measured by COSIMA on-board Rosetta. *Monthly Notices of the Royal Astronomical Society*, 2018, 477 (3), pp.3836-3844. 10.1093/mnras/sty560 . insu-02002394

HAL Id: insu-02002394

<https://insu.hal.science/insu-02002394>

Submitted on 8 Mar 2019

HAL is a multi-disciplinary open access archive for the deposit and dissemination of scientific research documents, whether they are published or not. The documents may come from teaching and research institutions in France or abroad, or from public or private research centers.

L'archive ouverte pluridisciplinaire **HAL**, est destinée au dépôt et à la diffusion de documents scientifiques de niveau recherche, publiés ou non, émanant des établissements d'enseignement et de recherche français ou étrangers, des laboratoires publics ou privés.

The oxygen isotopic composition ($^{18}\text{O}/^{16}\text{O}$) in the dust of comet 67P/Churyumov-Gerasimenko measured by COSIMA on-board Rosetta

J. A. Paquette,^{1★} C. Engrand,² M. Hilchenbach,¹ N. Fray,³ O. J. Stenzel,¹ J. Silen,⁴
J. Rynö,⁴ J. Kissel¹ and The Cosima Team

¹Max-Planck-Institut für Sonnensystemforschung, Justus-von-Liebig-Weg 3, D-37077 Göttingen, Germany

²Centre de Sciences Nucléaires et de Sciences de la Matière - CSNSM, CNRS/IN2P3-Univ. Paris Sud (UMR8609), Université Paris-Saclay, Bat. 104, F-91405 Orsay, France

³Laboratoire Interuniversitaire des Systèmes Atmosphériques (LISA), UMR CNRS 7583, Université Paris Est Créteil et Université Paris Diderot, Institut Pierre Simon Laplace, F-94000 Créteil, France

⁴Finnish Meteorological Institute, Observation services, Erik Palménin aukio 1, FI-00560 Helsinki, Finland

Accepted 2018 February 12. Received 2018 February 2; in original form 2017 November 16

ABSTRACT

The oxygen isotopic ratio $^{18}\text{O}/^{16}\text{O}$ has been measured in cometary gas for a wide variety of comets, but the only measurements in cometary dust were performed by the Stardust cometary sample return mission. Most such measurements find a value of the ratio that is consistent with Vienna Standard Mean Ocean Water (VSMOW) within errors. In this work we present the result of a measurement, using the COSIMA (the COmetary Secondary Ion Mass Analyser) instrument on the Rosetta orbiter, of the oxygen isotopic ratio in dust from Comet 67P/Churyumov-Gerasimenko. Measuring the $^{18}\text{O}/^{16}\text{O}$ ratio with COSIMA is challenging for a number of reasons, but it is possible with a reasonable degree of precision. We find a result of $2.00 \times 10^{-3} \pm 1.2 \times 10^{-4}$, which is consistent within errors with VSMOW.

Key words: comets: general – comets: individual: 67P/Churyumov-Gerasimenko – planetary systems.

1 INTRODUCTION

The oxygen isotopic ratio $^{18}\text{O}/^{16}\text{O}$ has been measured a number of times in cometary gas. For comet 1P/Halley, Balsiger, Altwegg & Geiss (1995) used mass spectrometry to determine the oxygen isotopic ratio in hydronium ions and in neutral water. Eberhardt et al. (1995), also using mass spectrometry, measured the ratio in neutral water. Both gave values consistent with the value for Vienna Standard Mean Ocean Water (hereafter VSMOW). This is also true for Biver et al. (2007), who measured the oxygen isotopic ratios in water for comets 153P/Ikeya–Zhang, C/2001 Q4 (NEAT), C/2002 T7 (LINEAR), and C/2004 Q2 (Machholz) in water using submillimetre astronomy, and for Bockelée-Morvan et al. (2012), who determined a value for water from comet C/2009 P1 (Garrad) using a far-infrared instrument. Hutsemékers et al. (2008) used ground-based ultraviolet spectroscopy to measure a ratio in OH (which comes from water) that was marginally higher than VSMOW for Comet C/2002 T7 and Decock et al. (2014) have a value that was significantly higher than VSMOW for comet C/2012 F6. These results are summarized in the review by Bockelée-Morvan et al. (2015).

More recently, measurements conducted on comet C/2014 Q2 (Lovejoy) using submillimetre astronomy showed an oxygen isotopic ratio in agreement with the terrestrial value (Biver et al. 2016). ROSINA measurements on water vapour from Comet 67P/Churyumov-Gerasimenko gave a ratio which was lower than the VSMOW value, but with large enough error bars that agreement cannot be precluded (Altwegg 2015). Of course, depending on the mechanism that fractionates the oxygen isotopes, there is no requirement for isotopic ratios measured in the gas to agree with a ratio measured in the dust.

Measurements of $^{18}\text{O}/^{16}\text{O}$ in cometary dust are much less common. The Stardust measurements of cometary dust from comet 81P/Wild 2 found most samples to have oxygen isotopic ratios in agreement with those typically measured in constituents of primitive meteorites (Nakamura et al. 2008; Nakashima et al. 2012; Ogliore et al. 2012). Calcium–aluminium-rich inclusions found in Stardust samples show the typical ^{16}O enrichment observed in primitive extraterrestrial material with regard to the terrestrial value (McKeegan et al. 2006; Simon et al. 2008; Nakashima et al. 2012). CAIs from meteorites typically range from $\delta^{18}\text{O} \approx \delta^{17}\text{O}$ of near zero down to about -50% . Ogliore et al. (2015) reported considerable variation in the oxygen isotopic ratios of fine-grained material encased in the walls of the Stardust sample tracks, ranging from values enriched in ^{16}O close to the Sun value (McKeegan et al. 2011) to heavy isotope

* E-mail: paquette@mps.mpg.de

enriched values similar to those measured in cosmic symplectite (Sakamoto et al. 2007).

This paper discusses the measurement of the $^{18}\text{O}/^{16}\text{O}$ ratio in cometary dust from Comet 67P/Churyumov-Gerasimenko (hereafter 67P). These measurements were made *in situ* using COSIMA (the COmetary Secondary Ion Mass Analyser) aboard the Rosetta spacecraft. Measuring the oxygen isotopic ratio with COSIMA is challenging for a number of reasons. First, this method must be undertaken in a negative mode, i.e. when COSIMA is set to collect negative ions, as the signal from oxygen in a positive mode is quite weak. In the negative mode, instrumental background effects are more of a difficulty than in the positive mode, and these effects must be accurately accounted for. Secondly, the interference at mass 18 from ^{17}OH must be taken into account. Thirdly, a very long measurement is needed to produce the necessary statistics for ^{18}O . Lastly, instrumental mass fractionation (hereafter IMF) must also be corrected for. Although the relative sensitivity factors in COSIMA for a number of elements have been determined (Krüger et al. 2015), the effect of IMF on the oxygen isotopic ratio has not been previously measured for this instrument. Thus, a measurement of the IMF had to be undertaken as a part of this work, using a sample of San Carlos olivine as a standard. While measurement of $^{17}\text{O}/^{16}\text{O}$ ratio would also be desirable, it is not possible to do so directly because of the strong interference at mass 17 from ^{16}OH that cannot be resolved with COSIMA (mass resolution of ~ 1000 at mass 100).

2 THE COSIMA INSTRUMENT

The COSIMA instrument on the Rosetta orbiter captured cometary dust on metal targets, imaged them, and then subjected some of the captured dust particles to Time of Flight Secondary Ion Mass Spectrometry (ToF-SIMS). In this technique, secondary ions ejected by the impact of an 8 keV beam of indium ions pass through a reflectron. The time of flight in such a system gives the mass per charge. Since most such ions have only one charge, the mass of the secondary ions is a direct result. COSIMA can be operated in a positive mode (in which positively charged secondary ions are collected and analysed) or in a negative mode (in which negatively charged secondary ions are collected and analysed). More complete descriptions of the COSIMA instrument are available in a number of papers (e.g. Kissel et al. 2007; Paquette et al. 2017).

One advantage of Rosetta over previous cometary missions (such as Stardust) is that Rosetta was not a flyby mission. The orbiter remained within tens to hundreds of kilometres of the nucleus of 67P, consequently the relative velocity of arriving cometary dust particles is much lower than it would be for a flyby mission, typically only a few metres per second (Rotundi et al. 2015) instead of kilometres per second. Consequently, the dust particles discussed here do not suffer compositional alterations due to high-speed impacts. Due to the temperature within the COSIMA instrument (10–15°C) ices not already lost in transit from the comet will be lost in the instrument (Hilchenbach et al. 2016).

3 MEASUREMENT TECHNIQUE

The counting rates for oxygen measurements in COSIMA in the negative mode are orders of magnitude greater than in the positive mode, so the negative mode must be used to obtain the necessary statistics. Even in the negative mode, ^{18}O is not plentiful, so a long measurement was necessary. A large particle named Jessica

Lummene.2 was selected for this measurement, and the results presented below pertain to this particle. The particle’s size was the initial reason for its consideration, but a more detailed rationale for its selection is given later in this section.

In the negative mode COSIMA spectra can contain instrumental artefact peaks (not seen in the positive mode) that must be corrected in order to obtain a meaningful result. To understand these effects, SIMS spectra were taken on a sample of San Carlos olivine that was placed on target 3C2 prior to launch. Fig. 1 shows portions of a COSIMA mass spectrum on the San Carlos olivine sample on target 3C2 in the negative mode in 2016 June.

Because of the size of COSIMA’s beam spot (about 35×50 microns full width at half maximum), the spectra shown are a mixture of signal originating from the olivine sample and from surface contamination (on the particle and on the gold substrate). The surface contamination is dominated by polydimethylsiloxane (PDMS), which is a surface contaminant with a high emission yield. To account for this, spectra taken on the target a few hundred microns away from the olivine were subtracted from the olivine spectra after normalizing to a fragment of PDMS at mass 75. For example, for ^{16}O :

$$^{16}\text{O}_{\text{olivine}} = ^{16}\text{O}_{\text{mixture}} - ^{16}\text{O}_{\text{target}} \times \left(\frac{^{75}\text{PDMS}_{\text{mixture}}}{^{75}\text{PDMS}_{\text{target}}} \right) \quad (1)$$

This gives a net contribution from the olivine sample with target contributions removed. Many rock-forming elements such as Mg are typically only visible in COSIMA positive mode spectra, and thus are not visible here. Positive mode spectra done on the olivine sample do show the expected peaks.

Fig. 1a shows a section of the spectrum from mass 1 to 200, with a few of the relevant peaks labelled. Fig. 1b shows a limited mass range of the spectrum around mass 16. The small peak to the left of the main one is due to an instrumental effect, resulting from the acceleration of secondary electrons from the reflectron exit grid. The main peak is due to ^{16}O . Fig. 1c has the same symbols as in Fig. 1b, but it shows the region around mass 17. The large peak contains a contribution from $^{17}\text{O}^-$, but is mainly due to $^{16}\text{OH}^-$. The small peak is an instrumental artefact due to secondary electrons as before. Fig. 1d shows the spectrum near mass 18. Due to the lower count rates, no secondary electron peak is visible. The main peak is mainly $^{18}\text{O}^-$, but contains a small contribution from $^{17}\text{OH}^-$, OD, and NH_4^- (as seen by the right shoulder on the peak).

The mineralogical and oxygen isotopic composition of San Carlos olivine is known, with $\delta^{18}\text{O} = 5.28\%$, or $^{18}\text{O}/^{16}\text{O} = 2.016 \times 10^{-3}$ (Kusakabe & Matsuhisa, 2008). Because SIMS disfavours the heavier oxygen isotope (Eiler, Graham & Valley 1997; Stephan 2001), the value of the $^{18}\text{O}/^{16}\text{O}$ ratio measured in COSIMA must be lower than the actual value due to IMF. The degree of fractionation is small, but can and must be accounted for.

Given the measured quantities and the previously measured composition, one needs only to assume that

$$\frac{^{17}\text{OH}}{^{17}\text{O}} = \frac{^{16}\text{OH}}{^{16}\text{O}} \quad (2)$$

and it becomes possible to calculate the $^{18}\text{O}/^{16}\text{O}$ ratio for San Carlos measured in COSIMA. This is done in the following manner. Given that the measured counts in the peak at mass 16 (P_{16}) are solely due to ^{16}O , and that the measured counts in the peak at mass 17 (P_{17}) are due to ^{16}OH and ^{17}O , and assuming that the measured counts in

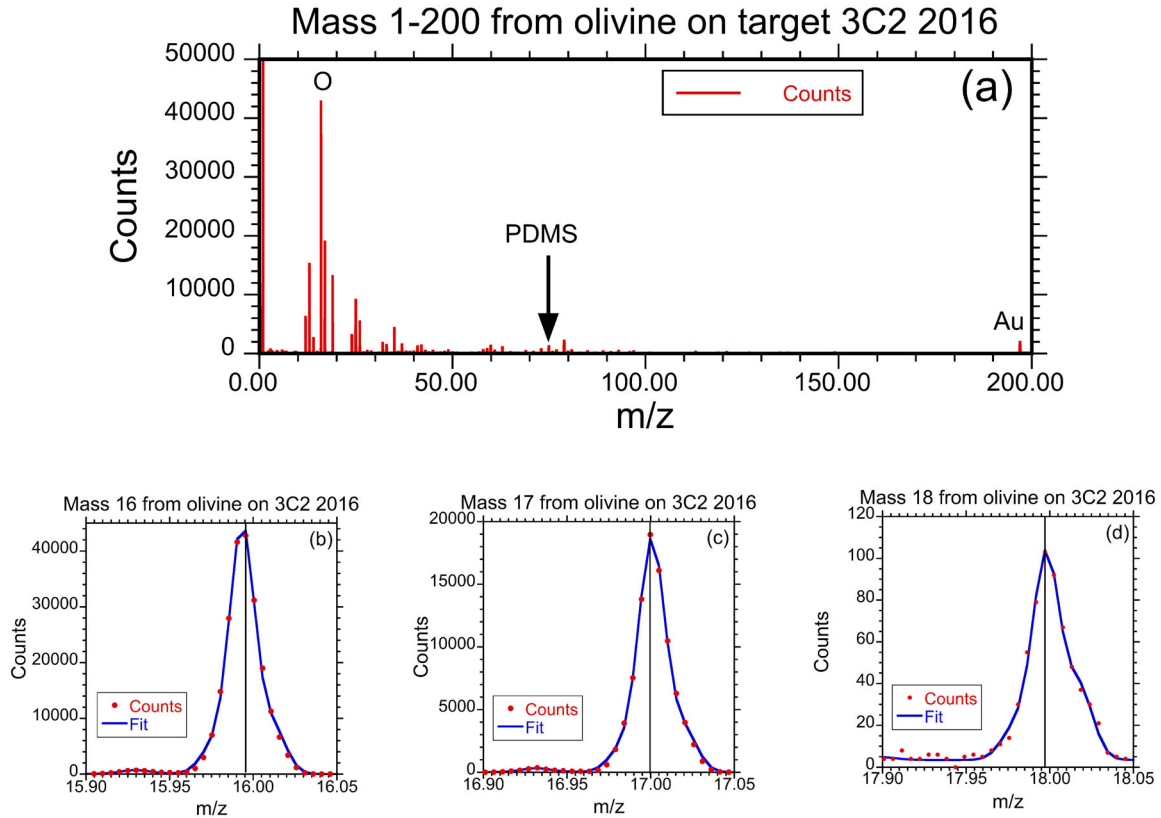


Figure 1. Sections of a COSIMA mass spectrum from ToF-SIMS (Time-of-Flight Secondary Ion Mass Spectrometry) on a sample of San Carlos olivine on target 3C2 in the negative mode. Note that the spectra shown in this figure include a contribution from the target as well as from the olivine. Also note that elements such as Mg are visible in positive spectra, and not visible here. Panel (a) shows a section of the spectrum from mass 1 to 200, with a few of the relevant peaks labeled. Panel (b) shows a smaller section of the spectrum around mass 16. The points are the data, the thick line is a multiple Gaussian fit using a Levenberg–Marquardt algorithm, and the thinner vertical line indicates where the fitting software found the peak. The small peak to the left of the main one is instrumental (due to the acceleration of secondary electrons from the reflectron exit grid). The main peak is due to ^{16}O . Panel (c) is as panel (b), but shows the region around mass 17. The large peak contains a contribution from ^{17}O , but is mainly due to ^{16}OH . The small peak is an instrumental artifact due to secondary electrons as before. Panel (d) shows the spectrum near mass 18. Due to the lower count rates, no electron peak is visible. The main peak is mainly ^{18}O , but contains small contributions from ^{17}OH and from OD, and an even smaller contribution from an instrumental effect (see the text).

the peak at mass 18 (P_{18}) are due to ^{18}O , ^{17}OH , and OD. Since the OD peak is given by

$$OD = \left(\frac{D}{H}\right) \text{OH} = \left(\frac{D}{H}\right) (P_{17} - ^{17}\text{O}) \quad (3)$$

then the $^{18}\text{O}/^{16}\text{O}$ ratio r_{18} is given by

$$r_{18} = \frac{P_{18} - r_{17}P_{17} + r_{17}^2P_{16} - \left(\frac{D}{H}\right)P_{17} + \left(\frac{D}{H}\right)r_{17}P_{16}}{P_{16}} \quad (4)$$

where $r_{17} = ^{17}\text{O}/^{16}\text{O}$.

The raw ratio r_{18} given by equation (4) for San Carlos olivine is 2.32×10^{-3} , which is far above the actual value, even though corrections for interferences from ^{17}OH and OD have been applied. In COSIMA's negative mode, spectra reliably contain instrumental peaks of electronic origin. These peaks are present in multiple spectra at the same time of flight. Thus the apparent excess in ^{18}O may be due to an instrumental peak which is superimposed with the ^{18}O peak. It is necessary to quantify this unseen electronic peak to accurately measure the oxygen isotopic ratio. While the San Carlos olivine spectra reveal the existence of this peak, they offer insufficient statistics to adequately quantify it. The same data used to compute the $^{18}\text{O}/^{16}\text{O}$ ratio on the olivine indicate that target 3C2 has an $^{18}\text{O}/^{16}\text{O}$ ratio that is compatible with VSMOW within errors. To get the necessary statistics, a long measurement on a target

is needed. Such a measurement was taken on target 2CF, also a gold target, in late 2016 March. The measurement was about 8 h in duration. The usual electronic peaks were visible in this spectrum as well. Fig. 2a shows the ^{18}O peak from this measurement and two other peaks (at masses 17.65 and 17.88, although they do not correspond to, or correlate with, any actual mass peak) which are instrumental artefacts. Fig. 2b shows the effect of subtracting the contribution from ^{18}O and ^{17}OH that must be present based on VSMOW leaving only the two instrumental artefact peaks that were visible in Fig. 2a and a third instrumental artefact peak that was obscured by the ^{18}O and ^{17}OH prior to their subtraction. Fig. 2c shows the electronic peak at 17.65 superimposed on the instrumental artefact peak at mass 18. No scaling has been done, simply a translation of the electronic peak in mass. The two peaks are nearly identical. This is not surprising, since small groups of very similar electronic peaks are seen at other points in the mass spectrum in the negative mode. This allows the determination of the invisible artefact peak, which contributes to the background for ^{18}O . It is the same size as the visible electronic peak at mass 17.65. This identity for the 2CF target spectrum should hold for the spectra on particle Jessica Lummene.2 on target 2CF also, for several reasons. First, the particle Jessica is located on target 2CF, secondly the spectra from particle Jessica were the next spectra taken after the 2CF background spectra (so there was only a matter of hours between the measurements), and

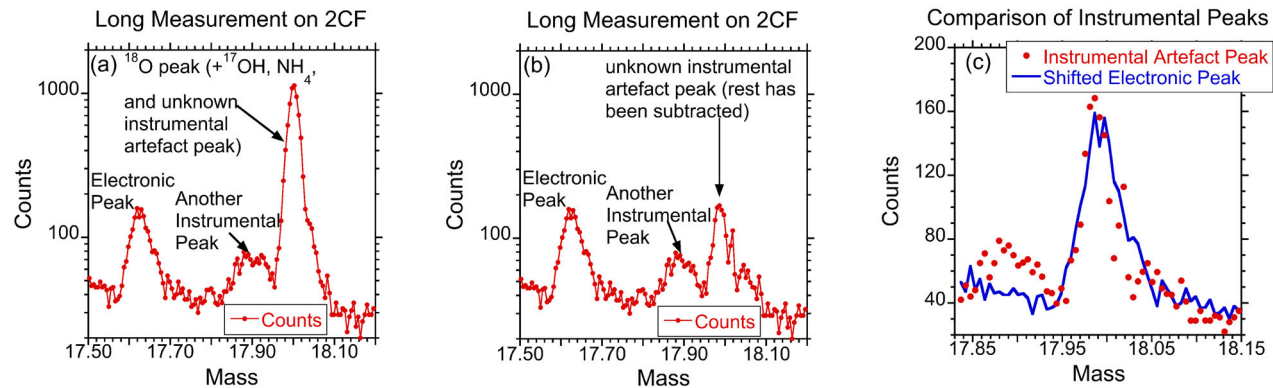


Figure 2. Long measurement was taken on the gold target 2CF in late March of 2016. Panel (a) shows the ^{18}O peak from this measurement and an electronic peak to the left of it around mass 17.65 (although it does not actually correspond to or correlate with any actual mass peak, it is an instrumental artifact). The low, wide peak at around mass 17.88 is another instrumental artifact, which scales with the total number of counts in the mass spectrum. Panel (b) shows the effect of subtracting the contribution from ^{18}O and ^{17}OH that must be present based on VSMOW, as well as a contribution from NH_4^- leaving only the instrumental artifact peak. Panel (c) shows the electronic peak at 17.65 superimposed on the instrumental artifact peak at mass 18. No scaling has been done, simply a translation of the electronic peak in mass. Examination suggests that the two peaks are nearly identical.

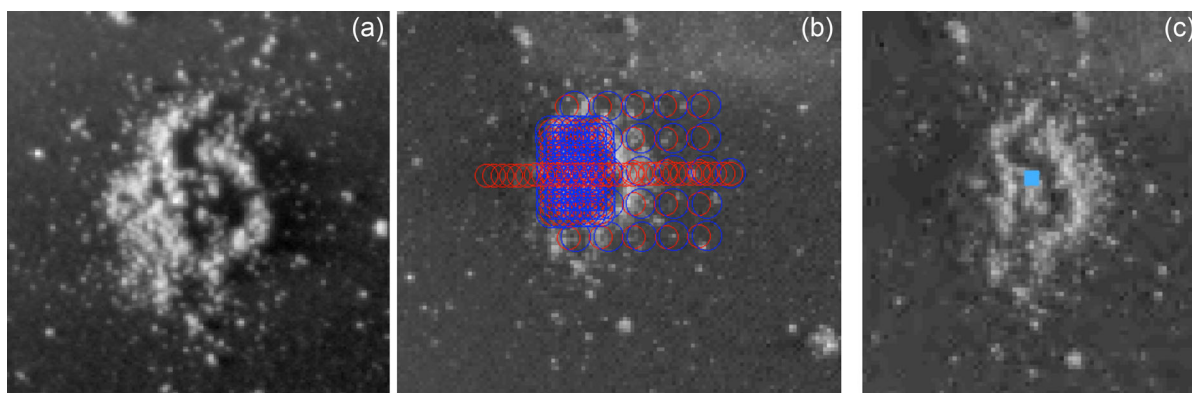


Figure 3. Three images of particle Jessica Lummene.2, a cometary dust particle collected by COSIMA on Target 2CF. Panel (a) (taken from Langevin et al. 2016) shows a Nyquist sampled image of Jessica (which is about 550 by 650 microns and 40 microns in height). Particle Jessica is considered to be a crossover between the shattered cluster and rubble pile categories (which are described in Langevin et al. 2016). Panel (b) shows the approximate locations of both positive (red circles) and negative (blue circles) spectra taken on Jessica before the very long measurement in 2016 April (see the text). The center of each circle indicates the rough center of the ion beam for the two spectra taken at each location. The four corners of the blue square shown in panel (c) indicate the four locations selected for the very long measurement.

thirdly the instrument settings were not changed between the two measurements. Thus the results from particle Jessica were corrected for these instrumental peaks.

Correcting for the instrumental peak in the olivine data measured in space gives an $^{18}\text{O}/^{16}\text{O}$ ratio which is 1.81×10^{-3} . Comparison between this value and the known $^{18}\text{O}/^{16}\text{O}$ ratio for San Carlos olivine gives an IMF of -102% .

Knowing the IMF of COSIMA for the measurement of oxygen isotopes, we can measure the $^{18}\text{O}/^{16}\text{O}$ ratio of the particle Jessica Lummene.2. COSIMA particles are named for ease of reference, with the second name (and digit, if any) indicating collection time (Merouane 2016). Particle Jessica was collected in 2015 January. Fig. 3a shows a Nyquist sampled image of the particle which is about 550×650 microns across and 40 microns high. Particle Jessica is considered to be a crossover between the shattered cluster and rubble pile categories (Langevin et al. 2016). Fig. 3b shows the locations of positive and negative spectra taken on particle Jessica prior to 2016 April. Fig. 3c depicts the four locations (the four corners of the blue square) that were chosen for a long measurement. Because the intensities of mass spectra from the dust particles are less than those from the substrate, a very long measurement was

needed to get the desired statistics – almost 48 h divided evenly among the four locations. This measurement was performed in early 2016 April.

The locations were selected by subjecting the spectra obtained from particle Jessica and the substrate to a Non-negative Matrix Factorization (hereafter NMF) analysis (Gillis & Vavasis 2014) to determine which locations had the greatest contribution of cometary signal and thus the lowest proportion of signal from the target substrate. This analysis decomposed a set of mass spectra at various locations on the particle Jessica and the target 2CF into two normalized spectra, and gave the amplitude of each normalized spectrum at each location. Thus the original spectra can be regarded as linear combinations of the two normalized spectra, i.e. the n^{th} spectrum in the set can be represented as

$$S_n \cong H_{1n} \times W_1 + H_{2n} \times W_2 \quad (5)$$

where H_{in} denotes the i^{th} coefficient of the n^{th} spectrum and W_i is the i^{th} -normalized spectrum. As shown in Fig. 4, one of the normalized spectra (W_1) was interpreted as being characteristic of the target due to substantial peaks at mass 75 (a fragment of PDMS which is a contaminant found on some COSIMA targets) and mass

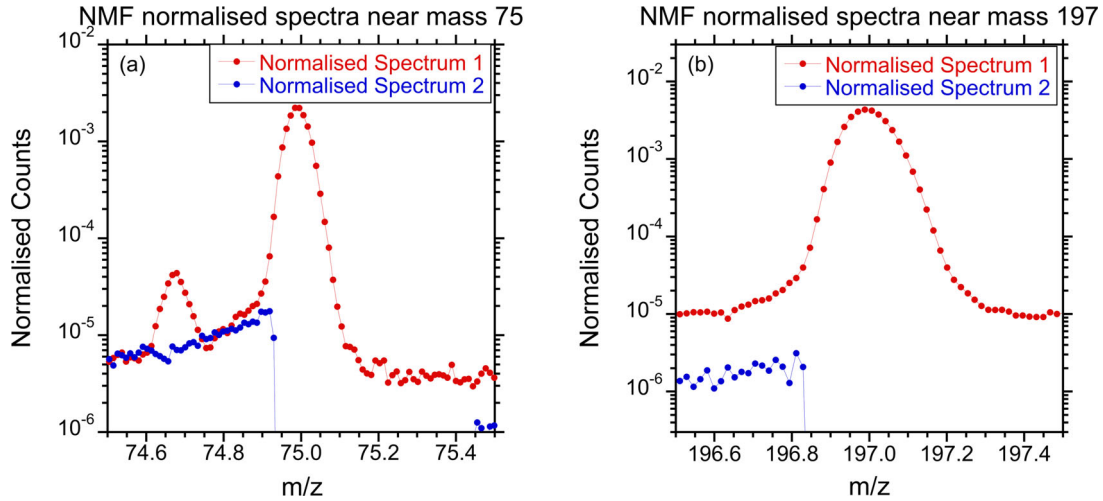


Figure 4. A Non-negative Matrix Factorization (NMF) analysis was done on a set of mass spectra taken on the dust particle Jessica Lummene.2 and its target substrate 2CF. NMF produced two normalised mass spectra, such that every mass spectrum in the original set could be written as a linear combination of these two normalised spectra. Panel (a) shows a section of the normalised spectra near mass 75. The main peak at this mass is a fragment of PDMS, a contaminant seen on some COSIMA targets. The smaller peak to the left is caused by electrons from the reflectron exit grid. Both of these peaks are strongly present in normalised spectrum 1, a sign that it is associated with the target. Panel (b) shows a section of the normalised spectra near mass 197. This peak is gold and comes from the target. Once again, this peak is strongly present in normalised spectrum 1, a sign that it is associated with the target. Thus we interpret normalised spectrum 2 as being more nearly cometary, and we used four locations where it alone was present for analysis.

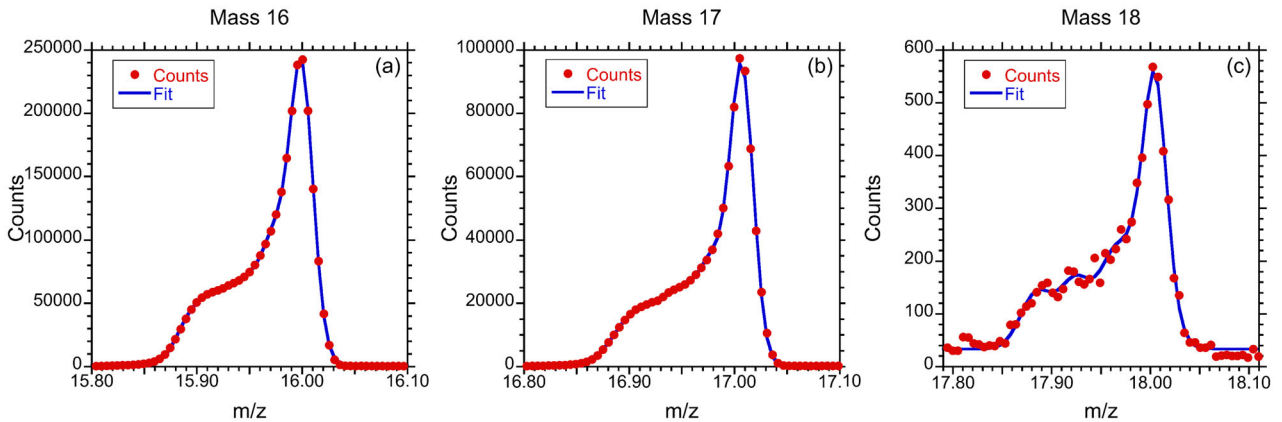


Figure 5. Sections of the mass spectrum resulting from the approximately 48 h of ToF-SIMS performed on the dust particle Jessica Lummene.2 on COSIMA target 2CF in 2016 April. Panel (a) shows the region around mass 16, panel (b) the region around mass 17, and panel (c) the region around mass 18. As before, the points are the data and the thick line is a Levenberg–Marquardt fit. In all three panels the points are the data and the line is a fit to that data. All three panels show a very pronounced leftward tail. In the negative mode this is a strong indication that the spectrum is coming from the dust particle rather than from the target substrate.

197 (gold, of which the target is composed). The other normalized spectrum (W_2) is very low near these contaminant peaks and was considered to be largely cometary in origin. The locations chosen were such that only W_2 was present there, i.e. H_{1n} corresponding to those locations were zero. This does not imply that spectra from these locations are totally cometary. The remaining contamination from the target had to be dealt with as described below. The spectra derived from the long measurement on Jessica have previously been used to determine the sulphur isotopic ratio (Paquette et al. 2017).

Sections of the spectrum that results from summing the mass spectra taken at these four locations are shown in Fig. 5. The three panels show the regions around masses 16, 17, and 18. Fits to peaks in COSIMA’s positive mode are often double or triple Gaussians, but obviously a more complicated functional form was needed to handle the unusual peak shape in the negative mode. In all three panels, a

very pronounced tail is visible on the left (low ToF) side of the main peak, a phenomenon peculiar to the negative mode. Such a tail can partly result from a topographic effect, as particle Jessica is about $40\ \mu\text{m}$ high, but the reach of the tail in these spectra could mostly result from alteration of the electric field that accelerates secondary ions into the reflectron by charging of the dust particle. The particle should be positively charged (due to the In^+ beam) and thus ions from the dust particle will be slower than ions from the target substrate, but simulations with the SIMION ion optics package show that these ions will take a shorter path in the reflectron, and thus, counterintuitively, will arrive first. While the mechanics of the creation of such a tail are not completely understood, empirically the presence of such a tail is a strong indication that the associated peak is coming from a cometary dust particle in many cases. On the particle Jessica the tail is extremely pronounced, and is present

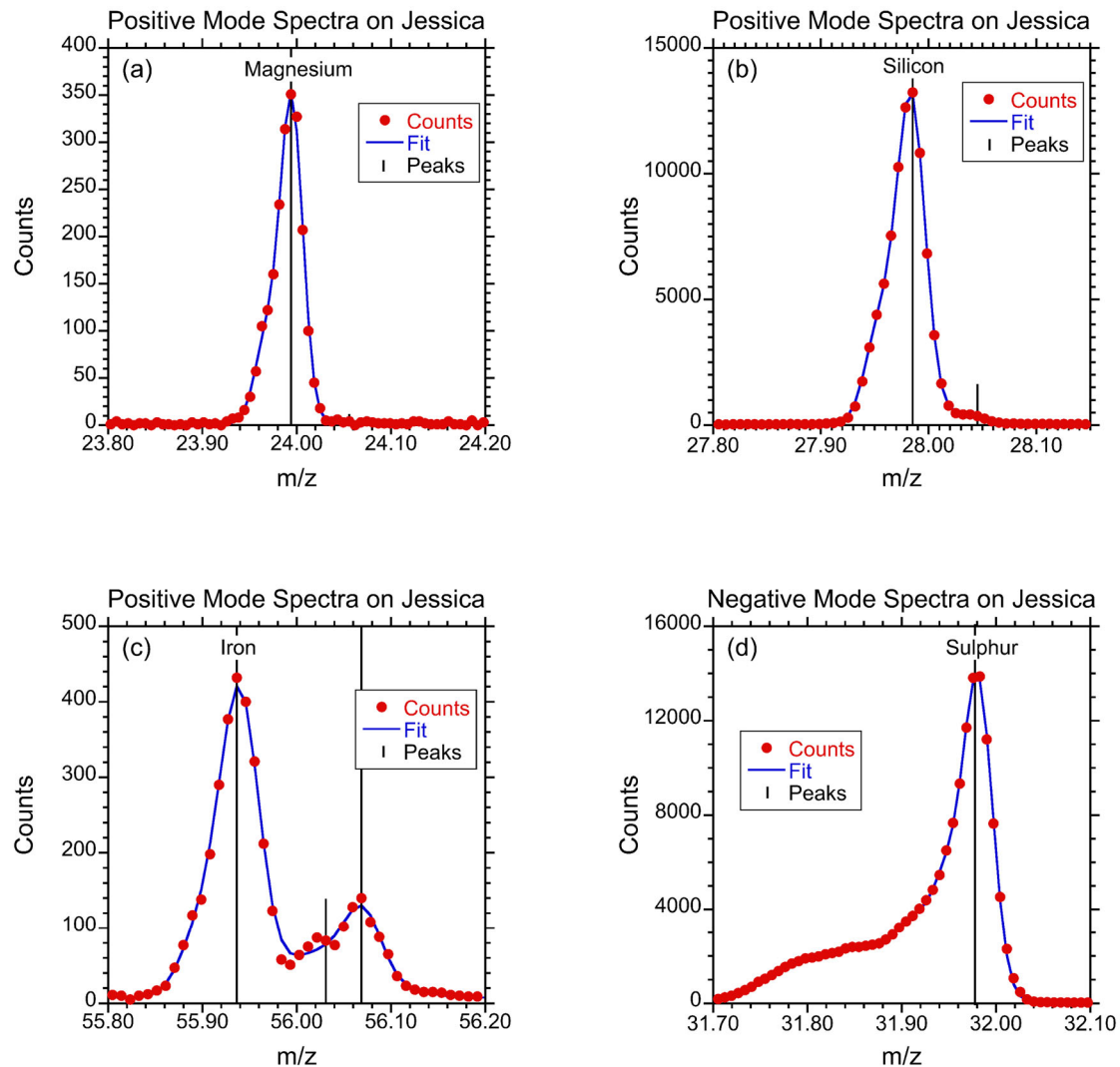


Figure 6. Three mass regions from the positive mode spectra taken on the same locations on Jessica where the oxygen isotopic analysis was done and one from the negative mode spectra. As before, the points are the data, the thick line is a fit, and the vertical lines indicate where the fitting routine found a peak. Panel (a) shows the presence of magnesium. Panel (b) shows the presence of silicon (the small peak to the right is an organic contaminant). Panel (c) shows the presence of iron (the two smaller peaks to the right are both organic contaminants). Panel (d) shows the presence of sulphur. Since it is from negative mode spectra (unlike the first three panels), it shows the characteristic left-side tail indicating that is from the particle rather than the substrate. This feature is absent in positive mode spectra.

to some degree on almost all peaks (except gold) but it is larger in peaks coming from the dust.

The main statistical error limit is imposed by the roughly 8600 counts in the peak at mass 18. The counts at mass 16 contribute a negligible amount to the final error.

Of course, these four points have some portion of their signal from the target substrate as well as from particle Jessica, so the technique of subtraction of background normalized to gold (described above) must be employed here as well. That technique indicates that 83–87 per cent of the counts (depending on mass) come from particle Jessica rather than from the substrate.

For all data corrections for the effects of IMF (-102%) were performed.

ToF-SIMS in the positive mode was also performed on the selected locations of particle Jessica. A few sections of the positive mode spectra (and one from the negative mode) are shown in Fig. 6. Fig. 6a shows the presence of magnesium at or near the locations on particle Jessica chosen for the oxygen isotopic measurements.

Fig. 6b shows that silicon is also present. Fig. 6c shows the presence of iron at the selected locations. The presence of magnesium, silicon, iron, and oxygen is consistent with the presence of silicates or amorphous silicates in particle Jessica. Some of the iron could be coming from iron sulphides rather than silicates, since sulphur is observed in the negative spectra (Fig. 6d; see also Paquette et al. 2017).

4 RESULTS

The $^{18}\text{O}/^{16}\text{O}$ isotopic ratio measured for particle Jessica is $2.00 \times 10^{-3} \pm 1.2 \times 10^{-4}$. It is shown in Fig. 7, where it is compared to other measurements of this ratio in comets as summarized in Bockelée-Morvan et al. (2015), to Stardust results (McKeegan et al. 2006), to Genesis results for the Sun (McKeegan et al. 2011), the range observed in CAIs, the VSMOW value, and the recent result from ROSINA (Altwegg 2015). Only dust measurements of the isotopic ratio are included in Fig. 7b. The COSIMA result agrees

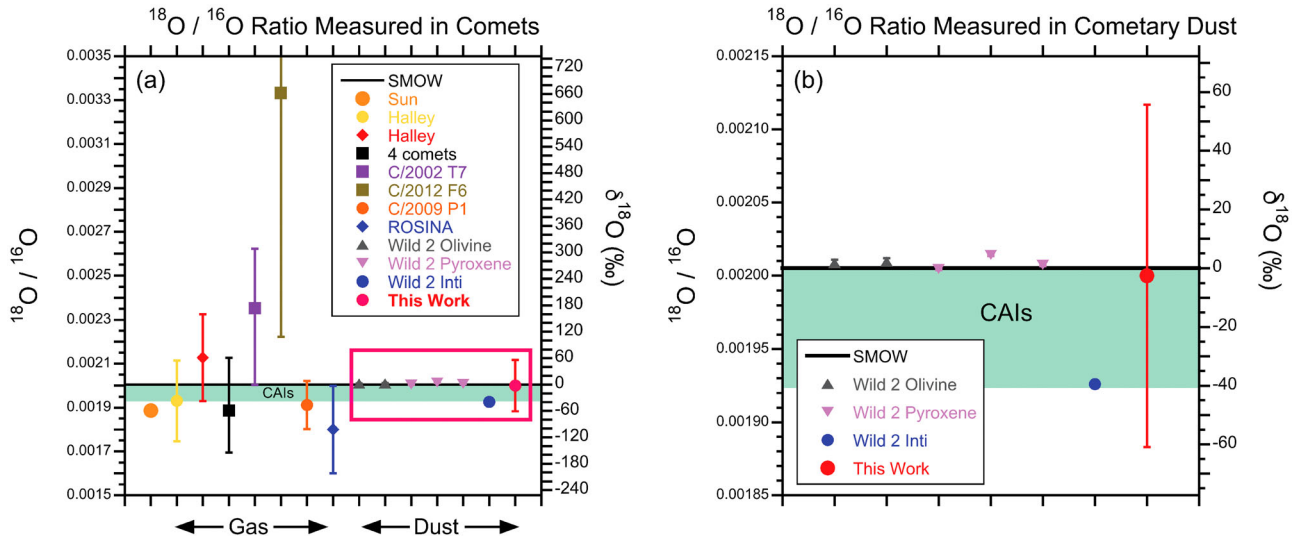


Figure 7. Comparison of previous measurements of the $^{18}\text{O}/^{16}\text{O}$ ratio in comets with the COSIMA measurement, with VSMOW and a typical range for Calcium Aluminum rich Inclusions (CAIs) shown for reference. Panel (a) shows a series of measurements of the oxygen isotopic ratio (taken from Bockelée-Morvan et al. 2015) together with Stardust samples (McKeegan et al. 2011), the recent measurement from Rosina (Altwegg 2015) and the result of this work. The Genesis result for the Sun (McKeegan et al. 2006) is plotted to the extreme left, then results measured in cometary gas, then results measured in cometary dust, with the result of this work plotted in red to the extreme right. The red box in panel (a) shows the region which is plotted at larger scale in panel (b). Only dust measurements of the isotopic ratio are included in panel (b). The COSIMA result agrees within errors with the VSMOW value, and with the Stardust values for olivine and pyroxene (taken from McKeegan et al. 2006). Obviously, the error for our measurement (which includes statistical errors and systematic errors added in quadrature) is much larger, but that is only to be expected given the limitations of space-based ToF-SIMS.

within errors with the VSMOW value. It also agrees with the Stardust values for olivine and pyroxene. Obviously, the error for our measurement (which includes statistical errors from counting statistics and systematic errors added in quadrature) is much larger, but that is only to be expected. The Stardust analysis was performed at leisure in a laboratory and thus with great precision. The COSIMA measurement was performed *in situ*, and is subject to the limitations of space-based ToF-SIMS – only a limited amount of time and resources (e.g. indium for the primary ion beam) can be spent on any one measurement, and instrumental effects cannot be as well constrained as in the laboratory.

In Fig. 8 the oxygen isotopic ratios from the four different locations at which measurements were performed are plotted along with the ratio derived from summing all four sets of spectra. In Fig. 8, the four locations are labelled with their target coordinates (x and y) in microns. The errors are naturally larger for individual locations as each has approximately a quarter of the statistics that the overall measurement has. Still, two of the locations show values that are consistent within errors with VSMOW, while the other two locations show values that are higher. In view of the size of the error bars, it is possible that the variation among the locations is merely statistical.

5 DISCUSSION

The oxygen isotopic composition of an extraterrestrial substance can serve as an indicator of the history of the material. While the bulk values of the Earth, Moon, and Mars are not far from the VSMOW value, the isotopic composition of chondrules in carbonaceous chondrites can be somewhat enriched in ^{16}O , with a $\delta^{18}\text{O}$ ranging down to -16% (Bridges et al. 2012). For calcium–aluminium-rich inclusions (CAIs) $\delta^{18}\text{O}$ can range down to -40% . There are several models to explain this, but the most popular is some form of photochemical self-shielding (e.g. Yurimoto &

Kuramoto, 2004). The Genesis measurements showed that $\delta^{18}\text{O}$ for the sun is about -60% (McKeegan et al. 2011). Presolar grains show very anomalous oxygen isotopic compositions, with a range of variations which is orders of magnitude greater. This diversity of isotopic compositions is attributed to nucleosynthetic processes (Sandford et al. 2008).

The previous measurements of the $^{18}\text{O}/^{16}\text{O}$ isotopic ratio in cometary dust have all been performed on samples returned by the Stardust mission to Comet 81P/Wild 2. In addition to the results from McKeegan et al. (2006) that are plotted in Fig. 7, there are a number of others.

In addition to the particle Inti (McKeegan et al. 2006; Simon et al. 2008), two other CAIs have been found in Stardust samples (Joswiak, Brownlee & Matrajt 2013). Compositional evidence for the presence of CAIs has been seen in comet 67P using COSIMA (Paquette et al. 2016). Measuring the oxygen isotopes at the locations where such evidence was seen was considered, but could not be performed because of operational difficulties.

Nakamura et al. (2008) found oxygen isotopic ratios in Stardust particles that were similar to those in meteoritic chondrules. Nakashima et al. (2012) found particles with oxygen isotopic ratios comparable to that of CAIs and Amoeboid Olivine Aggregates and also found compositions suggestive of chondrules. Ogliore et al. (2012) reported evidence for chondrule fragments in Stardust samples. Of course, the presence of such high-temperature phases in comets as CAIs and chondrules in comets suggests that relatively efficient transport of such materials to the outer solar system must have occurred.

Ogliore et al. (2015) analysed a set of 63 small (0.5–3 micron) particles from the bulb of a particular Stardust track. They found 10 particles with $\delta^{18}\text{O}$ that are comparable to those seen at the locations $X = 1090$, $Y = 4190$, and $X = 1120$, $Y = 4190$ on particle Jessica. Ogliore et al. (2015) concluded that the variations from VSMOW that they observed were not large enough to be indicative of presolar

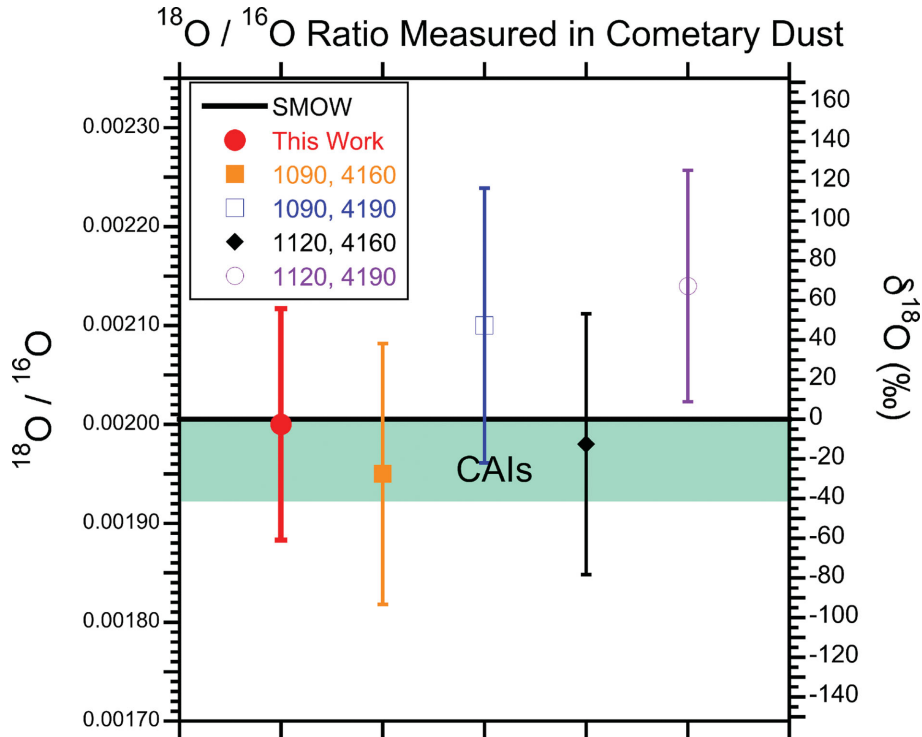


Figure 8. Comparison of the oxygen isotopic ration from the long measurement on Jessica Lummene.2 with the ratios from the four locations that comprised it, with VSMOW and a range typical of CAIs shown for reference. The locations are labeled by the relevant X and Y target coordinates in microns. The error bars of the ratios from individual locations are necessarily larger from simple statistical considerations. While the two ratios at Y = 4160 are somewhat lower than VSMOW, they agree with it within errors. The two ratios at Y = 4190 are somewhat higher than VSMOW.

grains. They offered two scenarios to explain the variations. In the first, such fine-grained material was formed in the inner nebula and efficiently transported outward to be incorporated into comets. In this scenario, the diversity of oxygen isotopic ratios arises from sampling of many different oxygen isotopic reservoirs. In the second scenario, the fine dust is representative of unequilibrated grains inherited from the solar system’s parent molecular cloud. Ogliore et al. (2015) were not able to distinguish between these two scenarios based on their measurements. Another point that these authors make is that the fine-grained dust that they analysed is not simply smaller versions of the larger grains. The fine-grained dust has a wider variation in oxygen isotopic composition than the large grains.

In addition to comparisons to Stardust samples, there are materials sampled on the Earth that are believed to be of cometary origin. These are the chondritic–porous anhydrous interplanetary dust particles (CP-IDPs) that have been collected in the stratosphere by NASA since the early eighties (e.g. Ishii et al. 2008), and the Ultracarbonaceous Antarctic Micrometeorites (UCAMMs) recovered from Antarctic snow (Duprat et al. 2010).

CP-IDPs mainly consist of Mg-rich olivines, pyroxenes, and iron sulphides (Bradley 2005), and they are rich in carbonaceous matter (Keller, Thomas & McKay 1994), which is also the case for the particles of 67P analysed by COSIMA (Fray et al. 2016). The bulk oxygen isotopic composition of CP-IDPs spans a range in $\delta^{18}\text{O}$ of about -20‰ to $+20\text{‰}$, (Starkey, Franchi & Lee 2014, and references therein), which is consistent within errors with what has been measured for the particle Jessica.

UCAMMs contain carbonaceous matter concentrations comparable to that of the most carbon-rich IDPs, although the UCAMM carbonaceous matter is more nitrogen-rich than that of CP-IDPs (Dartois et al. 2013). The oxygen isotopic composition

of UCAMMs is under investigation, but for two UCAMMs a $\delta^{18}\text{O}$ value of -5‰ was measured (Bockelée-Morvan et al. 2015; Kakazu et al. 2014). This agrees within errors with the results for particle Jessica.

While the data are consistent with silicates as the primary source of the cometary oxygen measured on particle Jessica, a definitive statement cannot be made on this point. Recently, evidence for the presence of carbonaceous matter on COSIMA dust particles has been found (Fray et al. 2016). This carbonaceous matter probably contributes some fraction of the measured oxygen. In ToF-SIMS, minerals usually have a higher emission yield than organic matter, but at present we cannot definitively determine what fraction of the oxygen that we observe comes from the carbonaceous matter.

6 CONCLUSIONS

Despite the presence of high-temperature components with very ^{16}O rich composition, and of large grain-to-grain variation, the bulk value for the $^{18}\text{O}/^{16}\text{O}$ ratio in cometary dust in Comet 61P/Wild 2 broadly agrees with VSMOW. Strong variations between comets (e.g. in the D/H ratio, Altwegg 2015) do occur, so repeating this measurement on dust from Comet 67P/Churyumov-Gerasimenko was necessary. This measurement for the dust particle Jessica Lummene.2 gives a result for the $^{18}\text{O}/^{16}\text{O}$ ratio for the dust particle Jessica Lummene.2 of $2.00 \times 10^{-3} \pm 1.2 \times 10^{-4}$, which agrees within errors with the terrestrial value.

When the four individual locations that went into the measurement are considered separately, a degree of variation between the isotopic ratios measured in each place is apparent. Based on statistical considerations, it is possible that the variation in the isotopic ratio is an actual spatial variation in the $^{18}\text{O}/^{16}\text{O}$ ratio. Similar

variations between dust particles have been seen, and this suggests that the dust that comprises particle Jessica is more similar to the fine-grained dust from a Stardust bulb measured by Ogliore et al. (2015) than it is to larger fragments also analysed in the Stardust sample.

ACKNOWLEDGEMENTS

COSIMA was built by a consortium led by the Max-Planck-Institut für Extraterrestrische Physik, Garching, Germany, in collaboration with Laboratoire de Physique et Chimie de l'Environnement et 8 de l'Espace, Orléans, France, Institut d'Astrophysique Spatiale, CNRS/Université Paris Sud, Orsay, France, Finnish Meteorological Institute, Helsinki, Finland, Universität Wuppertal, Wuppertal, Germany, von Hoerner und Sulger GmbH, Schwetzingen, Germany, Universität der Bundeswehr, Neubiberg, Germany, Institut für Physik, Forschungszentrum Seibersdorf, Seibersdorf, Austria, Institut für Weltraumforschung, Österreichische Akademie der Wissenschaften, Graz, Austria, and is led by the Max-Planck-Institut für Sonnensystemforschung, Göttingen, Germany. The support of the national funding agencies of Germany (DLR, grant 50 QP 1302), France (CNES), Austria, Finland, and the ESA Technical Directorate is gratefully acknowledged. We thank the Rosetta Science Ground Segment at ESAC, the Rosetta Mission Operations Centre at ESOC, and the Rosetta Project at ESTEC for their outstanding work enabling the science return of the Rosetta Mission.

REFERENCES

- Altwegg K., 2015, *Science*, 347, 1261952
- Balsiger H., Altwegg K., Geiss J., 1995, *J. Geophys. Res.*, 100, 5827
- Biver N. et al., 2007, *Planet. Space Sci.*, 55, 1058
- Biver N. et al., 2016, *A&A*, 589, A78
- Bockelée-Morvan D. et al., 2012, *A&A*, 544, L15
- Bockelée-Morvan D. et al., 2015, *Space Sci. Rev.*, 197, 47
- Bradley J. P., 2005, in *Meteorites, Comets and Planets: Treatise on Geochemistry*, Davis A. M., Holland H. D., Turevian K. K., eds, Elsevier-Pergamon, Oxford, p. 689
- Bridges J. C., Changela H. G., Nayakshin S., Starkey N. A., Franchi I. A., 2012, *Earth Planet. Sci. Lett.*, 341, 186
- Dartois E. et al., 2013, *Icarus*, 224, 243
- Decock A., Jehin E., Rousselot P., Hutsemékers D., Manfroid J., Cordier D., 2014, *Int. Comet Workshop*, Toulouse, France
- Duprat J. et al., 2010, *Science*, 328, 742
- Eberhardt P., Reber M., Krankowsky D., Hodges R. R., 1995, *Astron. Astrophys.*, 302, 301
- Eiler J. M., Graham C., Valley J. W., 1997, *Chem. Geol.*, 138, 221
- Fray N. et al., 2016, *Nature*, 538, 72
- Gillis N., Vavasis S. A., 2014, *IEEE Trans. Pattern Anal. Mach. Intell.*, 36, 698
- Hilchenbach M. et al., 2016, *Astrophys. J.*, 816, L32
- Hutsemékers D., Manfroid J., Jehin E., Zucconi J.-M., Arpigny C., 2008, *A&A*, 490, L31
- Ishii H. A., Bradley J. P., Dai Z. R., Chi M., Kearsley A. T., Burchell M. J., Browning N. D., Molster F., 2008, *Science*, 319, 447
- Joswiak D. J., Brownlee D. E., Matrajt G., 2013, *Meteorit. Planet. Sci.*, 48, A194
- Kakazu Y. et al., 2014, *Meteorit. Planet. Sci.*, 49, A195.
- Keller L. P., Thomas K. L., McKay D. S., 1994, in Zolensky M. E., Wilson T. L., Rietmeijer F. J. M., Flynn G. J. eds, *Analysis of Interplanetary Dust*. AIP Press, Woodbury New York, p. 159
- Kissel J. et al., 2007, *Space Sci. Rev.*, 128, 823
- Krüger H. et al., 2015, *Planet. Space Sci.*, 117, 35
- Kusakabe M., Matsuhisa Y., 2008, *Geochem. J.*, 42, 309
- Langevin Y. et al., 2016, *Icarus*, 271, 76
- McKeegan K. D. et al., 2006, *Science*, 314, 1724
- McKeegan K. D. et al., 2011, *Science*, 332, 1528
- Merouane S., 2016, *List of COSIMA Substrate Coordinate's Names*, Technical Report Max Planck Institute for Solar System Research, Göttingen, MPS-T-28-16-1
- Nakamura T. et al., 2008, *Science*, 321, 1664
- Nakashima D., Ushikubo T., Joswiak D. J., Brownlee D. E., Matrajt G., Weisberg M. K., Zolensky M. E., Kita N. T., 2012, *Earth Planet. Sci. Lett.*, 357, 355
- Ogliore R. C. et al., 2012, *Astrophys. J.*, 745, L19
- Ogliore R. C., Nagashima K., Huss G. R., Westphal A. J., Gainsforth Z., Butterworth A. L., 2015, *Geochim. Cosmochim. Acta*, 166, 74
- Paquette J. A., Engrand C., Stenzel O., Hilchenbach M., Kissel J., the COSIMA Team, 2016, *Meteorit. Planet. Sci.*, 51, 1340
- Paquette J. A., Hornung K., Stenzel O. J., Rynö J., Silen J., Kissel J., Hilchenbach M., the Cosima Team, 2017, *MNRAS*, 469, S230
- Rotundi A. et al., 2015, *Science*, 347, 6220
- Sakamoto N., Seto Y., Itoh S., Kuramoto K., Fujino K., Nagashima K., Krot A. N., Yurimoto H., 2007, *Science*, 317, 231
- Sandford S. A., Messenger S., DiSanti M., Keller L., Altwegg K., 2008, *Rev. Mineral. Geochem.*, 68, 247
- Simon S. B. et al., 2008, *Meteoritics Planetary Sci.*, 43, 1861
- Starkey N. A., Franchi I. A., Lee M. R., 2014, *Geochim. Cosmochim. Acta*, 142, 115
- Stephan T., 2001, *Planet. Space Sci.*, 49, 859
- Yurimoto H., Kuramoto K., 2004, *Science*, 305, 1763

This paper has been typeset from a Microsoft Word file prepared by the author.